18. Semm, P., Nohr, D., Demaine, C. & Wiltschko, W. Neural basis of the magnetic compass: interaction of visual, magnetic and vestibular inputs in the pigeon's brain. *J. Comp. Physiol. A* **155,** 283–288 (1984).
19. Semm, P. & Demaine, C. Neurophysiological properties of magnetic cells in the pigeon's visual system. *J. Comp. Physiol. A* **159,** 619–625 (1986).
20. Beason, R. C. & Semm, P. Magnetic responses of the trigeminal nerve system of the Bobolink (*Dolichonyx oryzivorus*). *Neurosci. Lett.* **80,** 229–234 (1987).
21. Hellmann, B. & Güntürkün, O. Structural organization of parallel information processing within the tectofugal visual system of the pigeon. *J. Comp. Neurol.* **429,** 94–112 (2001).
22. Diekamp, B., Hellmann, B., Troje, N. F., Wang, S. R. & Güntürkün, O. Electrophysiological and anatomical evidence for a direct projection from the nucleus of the basal optic root to the *nucleus rotundus* in pigeons. *Neurosci. Lett.* **305,** 103–106 (2001).
23. Mai, J. K. & Semm, P. Pattern of brain glucose utilization following magnetic stimulation. *J. Hirnforsch.* **31,** 331–336 (1990).
24. Güntürkün, O. & Hahmann, U. Functional subdivisions of the ascending visual pathways in the pigeon. *Behav. Brain Res.* **98,** 193–201 (1999).
25. Batschelet, E. *Circular Statistics in Biology* (Academic, London, 1981).

Acknowledgements

This work was supported by grants from the Deutsche Forschungsgemeinschaft. We thank K. Dutine, F. Eich, F. Schmidt and A. Wittekindt for their help with conducting the experiments.

Competing interests statement

The authors declare that they have no competing financial interests.

Correspondence and requests for materials should be addressed to W.W. (e-mail: wiltschko@zoology.uni-frankfurt.de).

Moving visual stimuli rapidly induce direction sensitivity of developing tectal neurons

Florian Engert*†‡, Huizhong W. Tao*†, Li I. Zhang†§ & Mu-ming Poo*

* *Division of Neurobiology, Department of Molecular and Cell Biology, University of California, Berkeley, California 94720, USA*
§ *Keck Center of Integrative Neuroscience, University of California, San Francisco, California 94143, USA*
† *These authors contributed equally to this work*

During development of the visual system, the pattern of visual inputs may have an instructive role in refining developing neural circuits[1–4]. How visual inputs of specific spatiotemporal patterns shape the circuit development remains largely unknown. We report here that, in the developing *Xenopus* retinotectal system, the receptive field of tectal neurons can be 'trained' to become direction-sensitive within minutes after repetitive exposure of the retina to moving bars in a particular direction. The induction of direction-sensitivity depends on the speed of the moving bar, can not be induced by random visual stimuli, and is accompanied by an asymmetric modification of the tectal neuron's receptive field. Furthermore, such training-induced changes require spiking of the tectal neuron and activation of a NMDA (*N*-methyl-D-aspartate) subtype of glutamate receptors during training, and are attributable to an activity-induced enhancement of glutamate-mediated inputs. Thus, developing neural circuits can be modified rapidly and specifically by visual inputs of defined spatiotemporal patterns, in a manner consistent with predictions based on spike-time-dependent synaptic modification.

Spontaneous and experience-evoked activities in the developing brain can influence the refinement of developing nerve connections into mature neural circuits. In the visual system, rearing kittens with an artificial squint leads to failure in the development of binocular response properties of striate cortex neurons[5]. Blockade of spontaneous waves of retinal activity also disrupts eye-specific segregation of retinal inputs to the lateral geniculate nucleus[6,7]. Synchronizing retinal inputs by strobe light or electrical stimulation affects formation of normal receptive field properties in various systems[8–10]. Furthermore, an instructive role of visual inputs is indicated by the appearance of visual modules in the auditory cortex of the ferret after rewiring of retinal inputs[11,12]. In the present study, we found a rapid and specific modification of receptive field properties of tectal neurons by the visual input of a defined spatiotemporal pattern, in a manner consistent with hebbian synaptic modification as a mechanism for activity-dependent changes in visual circuits[13,14].

The effect of visual experience on the receptive field properties of tectal neurons was examined in developing *Xenopus* tadpoles. Patterned visual inputs were used to stimulate the retina, and tectal cell responses were monitored with *in vivo* perforated whole-cell recording methods (Fig. 1a). First, we mapped the receptive field of the tectal neuron by random and sequential flashing of a white square at various locations on the retina (see Methods). The integrated charge of stimulus-evoked compound synaptic currents (CSCs) was measured within a defined window for the more prominent 'off' responses (Fig. 1b). The measured value at each location was represented in grey scale as one element of an 8×7 grid that covered the total area of the projected visual image on the retina (Fig. 1c). This analysis based on CSCs reveals a large receptive field (50–80% of the retina, $n = 12$) of tectal neurons at these early stages (42–45), consistent with a diffuse retinotectal connectivity during early development[15,16].

To examine the effect of patterned visual inputs on the receptive field property of tectal neurons, we stimulated the retina with white moving bars (20-μm wide, speed 0.3 μm ms^{-1}) in four orthogonal directions (right, down, left and up, Fig. 2a) and recorded the responses of tectal cells evoked by moving visual stimuli. In all tectal cell responses (voltage-clamped at −70 mV, $n = 20$), we found no

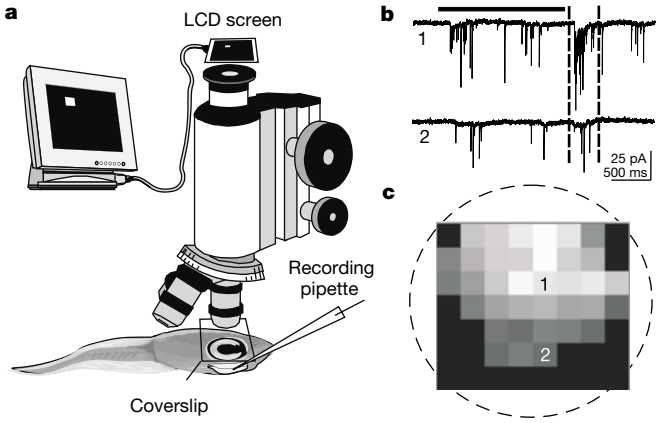

Figure 1 Mapping the receptive field of developing *Xenopus* tectal neurons. **a**, Diagram of the experimental set-up, depicting the recording of a tectal neuron in the exposed tectum. **b**, Traces shown are samples of compound synaptic currents (CSCs) evoked by the flashing of a white square (for 1.5 s, bar) within the receptive field at two locations (marked 1 and 2). Recording was made in voltage clamp at the reversal potential of Cl^- current (−45 mV) to reveal glutamate-mediated inputs. **c**, The receptive field was assayed by measuring the integrated charge of the 'off' response of CSCs within a defined window (dotted lines in **b**). The value of CSC charge is represented by linear grey scale (black = average basal activity without light stimulus) as a corresponding element in the 8×7 grid covering the projection area. The dashed circle marks the approximate position of the retina.

‡ Present address: Department of Molecular and Cell Biology, Harvard University, Cambridge, Massachusetts 02138, USA.

apparent directional preference to moving bars in any of the four directions, in terms of the total charge of CSCs evoked by each moving stimulus (see Fig. 2b, green bars), although these CSCs exhibited a distinct profile for each direction (Fig. 2a). As these developing tectal neurons had no apparent directional preference, we inquired whether repeated exposure of directional stimuli can 'train' these neurons to acquire direction-sensitivity in their responses. After the initial assay of tectal cell responses to moving-bar stimuli in each of the four directions (voltage-clamped at −70 mV), the recording was switched to current clamp and the retina was exposed to 60 sweeps of the moving bar (speed 0.3 μm ms^{-1}, frequency 0.2 Hz) in one specific, but randomly chosen, direction (rightward in Fig. 2). In many neurons, each sweep elicited reliably a train of spikes (Fig. 2b, inset). When the tectal cell responses were assayed again after the training, we found that the response to the training stimulus (bar to the right in Fig. 2a) was enhanced to a level significantly larger than those for other directions. In Fig. 2a, the effect is further illustrated by superimposing the current traces before and after training for each direction. The enhancement of CSCs also led to an increased spike rate of the tectal neuron in response to the training stimulus (Fig. 2c). In most experiments, we monitored CSCs (in voltage clamp) instead of spiking activities to avoid spiking-dependent changes caused by testing. Figure 2d depicts the time course of training-induced changes in seven experiments, for which the training stimulus reliably induced spiking of the tectal cell. The enhancement of tectal cell response to the test stimulus of the trained direction was persistent for up to 50 min.

In many regions of the developing brain[14,17–20], the timing of spiking in pre- and postsynaptic neurons is critical for the induction of long-term potentiation (LTP) and long-term depression (LTD). Modelling studies indicate that such spike-time-dependent plasticity may provide a mechanism for the development of direction-selectivity of visual circuits for detecting moving stimuli[21–24]. Moving bars probably evoke consecutive spiking of neighbouring retinal ganglion cells and of the tectal cells they innervate, with specific temporal relationships. Such a spatiotemporal pattern of spiking may be essential for triggering synaptic changes underlying the development of direction-selectivity. We further tested this idea by using bar stimuli that moved at slower speeds. As shown in Fig. 3a,

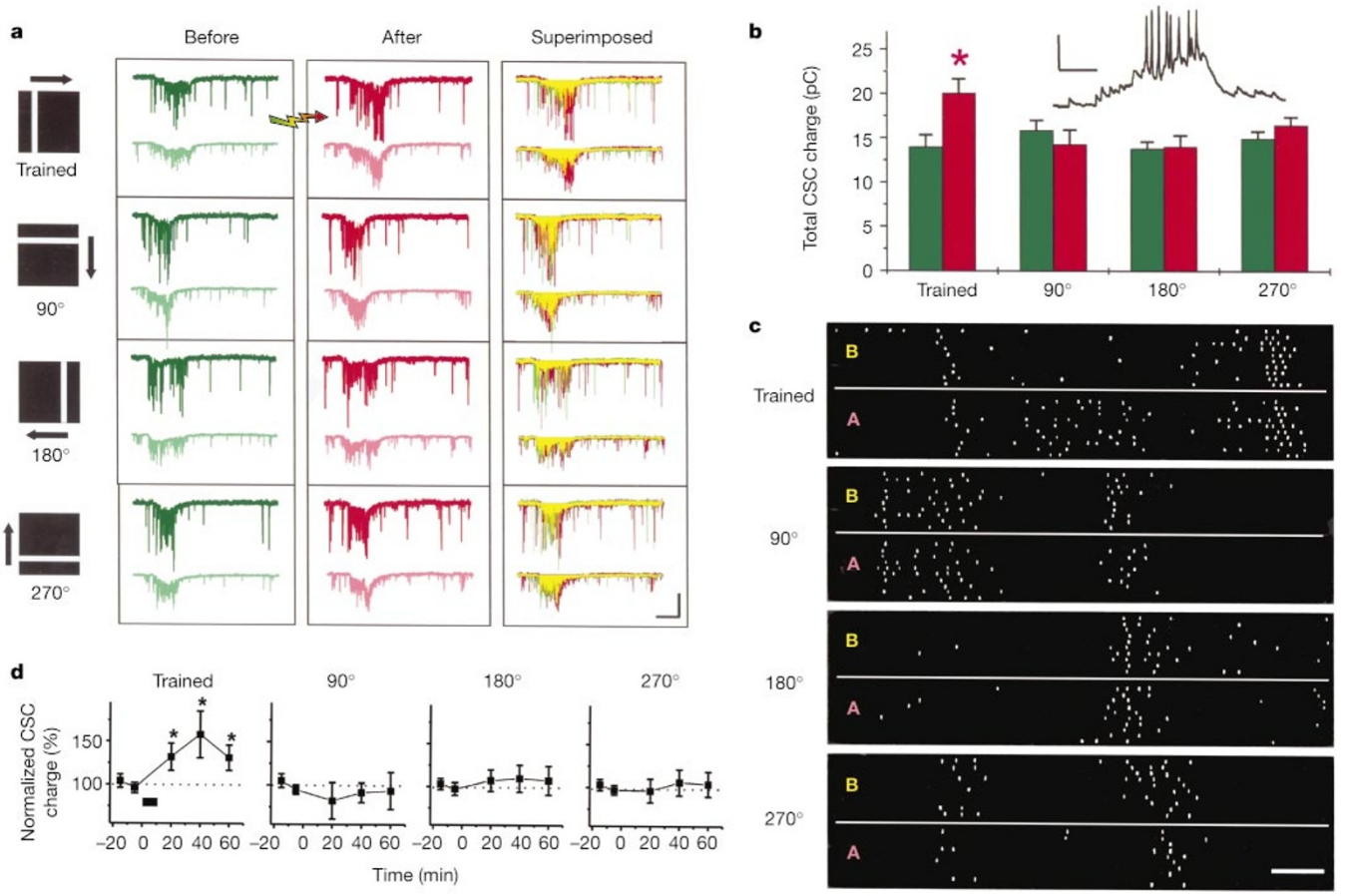

Figure 2 Selective enhancement of tectal cell responses by training with a moving bar. **a**, Traces of CSCs evoked by test moving bars of four orthogonal directions before (green) and after (red) repetitive exposure of the retina to rightward moving bars (coloured arrow). Bright traces indicate CSCs evoked by a single test sweep; dim traces indicate averages of three CSCs. Superimposed traces reveal the enhanced tectal response for the trained direction (see red area). Scale bar: 50 pA (vertical), 500 ms (horizontal). **b**, Average total CSC charge (±s.e.m., $n = 6$) evoked by the moving stimulus before (green) and after (red) training, for the experiment shown in **a**. The average CSC charge for the trained direction was significantly enhanced, as compared with either its value before training or after-training values for all three other directions (asterisk, $P < 0.02$, two tailed t-test). Inset, sample trace of tectal cell response evoked by the training stimulus (in current clamp, $V_m = -50$ mV). Scale bar: 20 mV (vertical), 300 ms (horizontal). **c**, Training-induced changes in the stimulus-evoked spiking activity of the tectal neuron. Raster plots show spike trains evoked by ten consecutive test moving stimuli before (B) and after (A) the training (as in **a**), with each white dot depicting a spike. Scale bar, 100 ms. **d**, Persistency of training-induced, direction-sensitive tectal responses ($n = 7$). Training was performed at 0–10 min (black bar). Data from each experiment were normalized to the average pre-training control and pooled into five bins. Asterisk, significantly different from the corresponding data for other directions ($P < 0.05$, paired t-test).

no significant direction-specific change was induced by training with the slow-moving bar (0.1 μm ms^{-1}), whereas bars moving with a medium speed (0.2 μm ms^{-1}) induced a slight increase in the tectal response to the training stimulus. Comparing the patterns of tectal spikes, we found that the fast bar generated spikes with significantly shorter inter-spike intervals (Fig. 3d), although the total number of spikes evoked by each sweep was the same (5.4 ± 0.8 and 5.6 ± 0.7 for the fast and slow sweeps, respectively). Thus the timing of sequential excitation of retinal cells seems to be critical for inducing direction-specific changes in the tectal neurons. In addition, we found that after training with the fast-moving bar, the tectal response became enhanced only for the test bar that moved at the fast but not the slow speed (Fig. 3b). Thus the circuit modification depends on the speed of the training stimulus, and the modified circuit is specific for the detection of the training stimulus.

The importance of the spatiotemporal pattern of retinal excitation in the observed training effects was further examined by exposing the retina to randomized training stimuli. We used non-overlapping white squares that flashed in random sequence and covered the same area of the visual field for the same amount of time as the fast-moving bar stimulus (Fig. 3c). Each set of random flashes evoked a similar total number of spikes (5.3 ± 0.7) as that by a sweep of the fast-moving bar, but the distribution of inter-spike intervals was significantly different, with spikes dispersed over longer intervals (Fig. 3d). After training with 120 sets of random flash stimuli, we found no enhancement of tectal responses in any direction (Fig. 3c). Thus the pattern of spiking, presumably in both pre- and postsynaptic neurons, is critical in the observed induction of direction-sensitive responses. Finally, we tested the effect of training with bars of four orthogonal directions, with a random sequence of occurrence but the same number (60) of sweeps for each direction. We found that the tectal responses after the training were enhanced in all four directions (Fig. 3c), although the level of enhancement was lower than that induced by the unidirectional training. Thus the tectal cell is not pre-determined to be direction-selective in a particular direction. The appearance of direction-selectivity *in vivo* presumably requires an imbalance of moving visual stimuli and other mechanisms for consolidating the acquired response properties of the tectum.

To explore cellular changes induced by the training stimuli, we examined further the receptive fields of tectal cells before and after training. To facilitate rapid mapping, we used a set of ten vertical and ten horizontal flashing bars in random sequence to determine the receptive field profiles of the tectal neuron in horizontal and vertical directions, respectively (Fig. 4a). After training with fast bars in one direction, an asymmetric change in the profile of the tectal receptive field was revealed by the enhanced tectal cell responses only for upstream test bar locations (Fig. 4a). As sum-

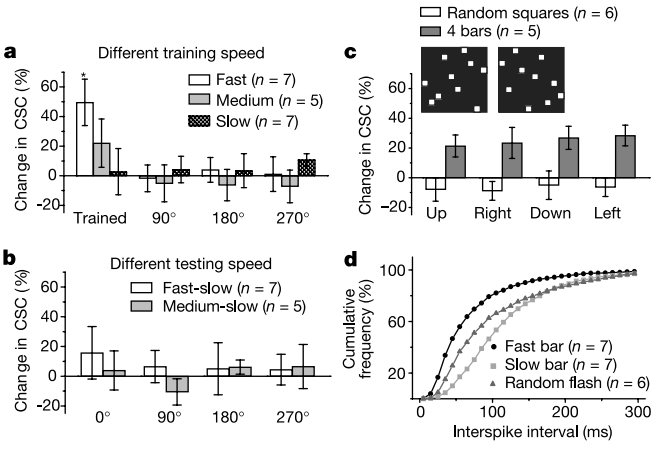

Figure 3 Effect of training with stimuli of different spatiotemporal patterns. **a**, Percentage changes in the total CSC charge for responses to moving bars in four test directions after training with three different speeds. Data (mean ± s.e.m.) within 30 min after training were averaged and normalized to the pre-training control. The same speed of the moving bar was used for training and testing. Asterisk, significantly different from other test directions ($P < 0.01$, *t*-test). **b**, Normalized responses to slow test bars after training with the fast-(fast–slow) or the medium-speed (medium–slow) moving bar, respectively. 0°, test direction the same as the training direction. **c**, Results of training with random flashing squares (white, see insets for two examples of the image) and with four orthogonal moving bars in random sequence (grey). **d**, Cumulative distribution of inter-spike intervals for tectal cell spikes during training in response to a sweep of the fast- or slow-moving bar, or an equivalent set of random flashing squares.

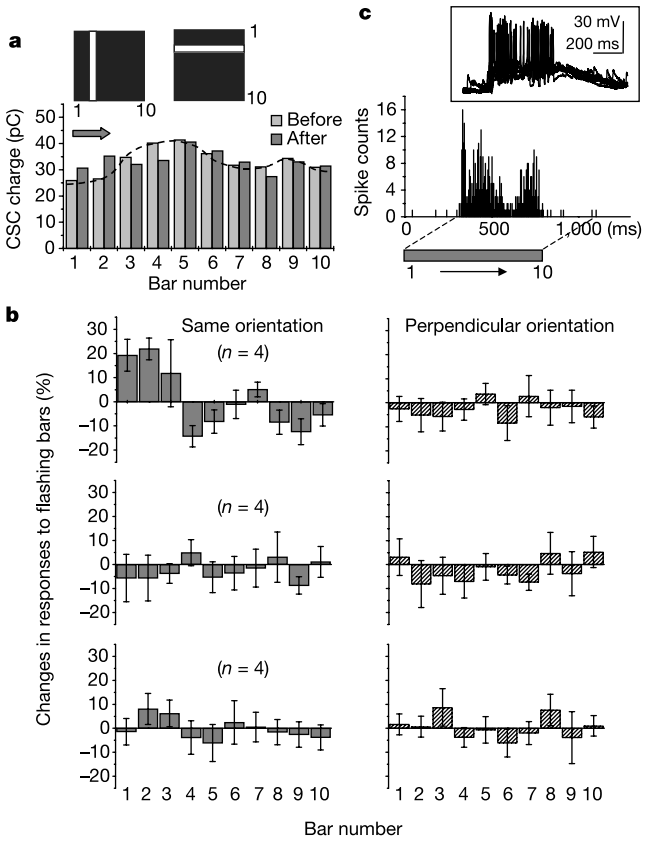

Figure 4 Asymmetric modification of the tectal receptive field by training with moving stimuli. **a**, Average CSC charge of tectal cell responses (eight repeats) to a set of ten vertical flashing bars (labelled 1–10 along the training direction, each flashed for 1.5 s, left inset) before and after training with fast (rightward, arrow) moving bars. Dashed curve, receptive field profile before training. The receptive field profile was also determined for the perpendicular dimension by measuring the tectal responses to horizontal bars (numbered 1–10 along the direction that was 90° clockwise to the training direction, right inset box; data not shown). Recordings were made at the reversal potential of Cl^- currents. **b**, Top panel, summary of four experiments similar to **a**. Histograms depict the mean percentage changes after training in tectal responses to flashing bars of the same (grey) and perpendicular (hatched) orientation with respect to the training direction. The middle panel is the same as the top panel except that the tectal cell was hyperpolarized constantly (at −80 mV in current clamp) and prevented from spiking during training. The bottom panel is the same as the top panel except that the training stimulus was the slow-moving bar. **c**, Post-stimulus spike-timing histogram for tectal responses during the training for the experiment shown in **a**. The onset of the moving stimulus on the screen was set as time 0, and it took about 700 ms for the bar to sweep across the visual field (bar below). The left dashed line marks the onset of the stimulus-evoked synaptic potential with respect to the onset of the stimulus. Inset, superimposed tectal potentials (six samples) during training.

marized in Fig. 4b (top panel), asymmetric receptive field modification was induced by fast-moving bars along the direction of the movement, whereas no apparent asymmetry was found for receptive field in the perpendicular dimension. This is analogous to the asymmetric change in hippocampal place field induced by unidirectional movement of a rat in a closed track[25], which is consistent with the prediction by a computational model based on asymmetric spike-time-dependent synaptic modification[26]. Spiking of tectal neurons evoked by the fast-moving bar appears with a delay of a few hundred ms after the onset of the stimulus sweep on the projection screen (Fig. 4c), with most spikes clustered during the early phase of the sweep, where modification of the receptive field was most prominent. In addition, consistent with the involvement of spike-time-dependent plasticity, no change in the receptive field profile was observed when the tectal cell was hyperpolarized to be prevented from spiking during training (Fig. 4b, middle panel), or when the slow-moving bar was used for training (Fig. 4b, bottom panel).

Direction-sensitive tectal responses induced by training may result from changes in the tectum or in the retina. We found that when unidirectional fast-bar training was performed under voltage clamp (−80 mV) of the tectal neuron, there was no significant change in the responses of tectal neurons to stimuli in any of the four directions (Fig. 5a). In three experiments, two training sessions were given sequentially, with the tectal cell in voltage clamp (−80 mV) and then in current clamp. Post-training tests showed no change in the tectal responses after training in voltage clamp (−10% ± 10, s.e.m.), but a significant enhancement after training in current clamp (48% ± 11%). Thus the induction of direction-sensitive responses required depolarization of the tectal cell. Furthermore, training stimuli that consistently failed to elicit spike trains in the tectal cell did not induce responses with

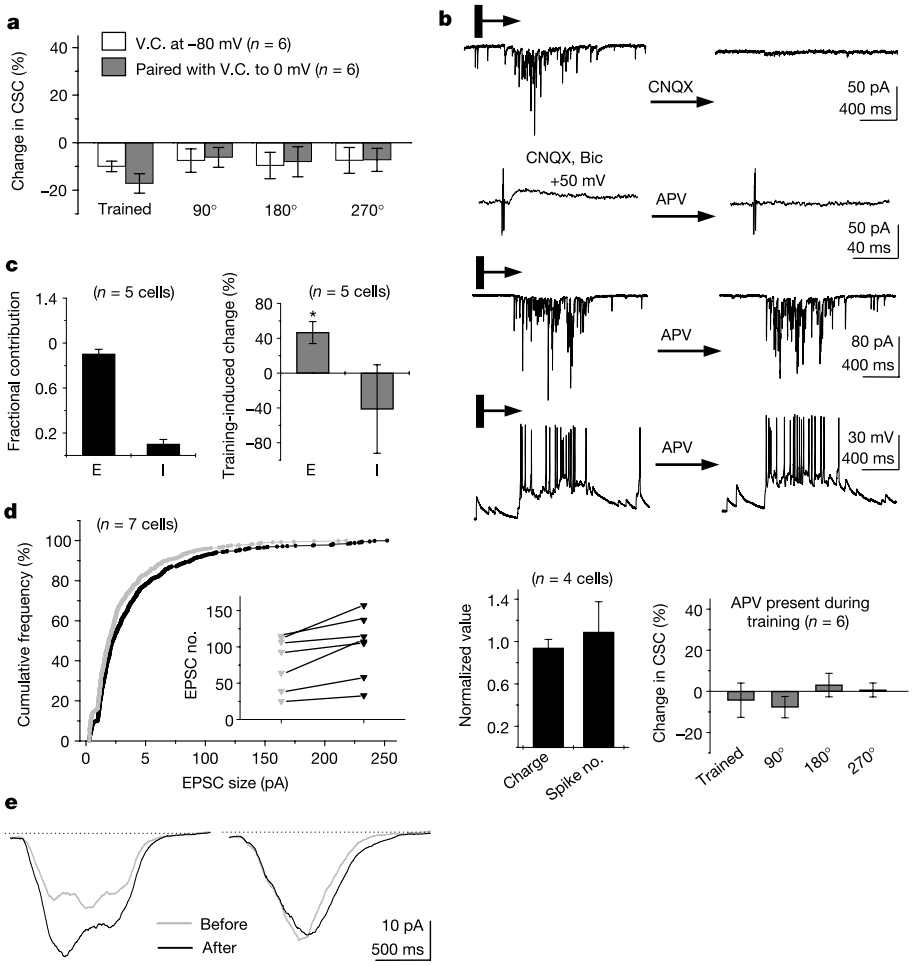

Figure 5 Synaptic mechanisms. **a**, Experiments similar to Fig. 2a except that during training the tectal cell was voltage-clamped (v.c.) at −80 mV (white) or depolarized from −70 to 0 mV for 700 ms during each training sweep (grey). **b**, The top upper panel shows sample traces of CSCs evoked by a moving bar before and after local perfusion of the tectum with CNQX. The top lower panel shows NMDA receptor-mediated synaptic currents (voltage-clamped at +50 mV) induced by electrical stimulation of the retina (with CNQX and bicuculline in the bath) before and after local perfusion with D-APV. The middle panel shows sample traces of moving-bar-induced CSCs and spikes before and after local perfusion with D-APV. The bottom left panel shows the average total CSC charge and spike number evoked by the moving-bar stimulus after D-APV perfusion, normalized for each cell to the pre-perfusion value. The bottom right panel shows the average percentage changes (±s.e.m) in the CSC charge of responses to fast-moving bars after training, with D-APV present during training. **c**, Fractional contribution of Na^+ (excitatory (E)) and Cl^- currents (inhibitory (I)) in the CSCs evoked by the moving-bar stimulus (left). Training-induced changes in the 'E' and 'I' components of CSCs (asterisk, $P < 0.01$, *t*-test) (right). **d**, Cumulative distribution of the amplitude of individual EPSCs associated with the CSCs evoked by the moving bar of the trained direction before (light) and after (dark) training. The two curves are significantly different ($P < 0.01$, Kolmogorov–Smirnov test). Inset, the total number of EPSCs associated with the same CSCs before (grey) and after (black) training. Lines connect data points from the same experiment. Two groups are significantly different ($P < 0.01$, paired *t*-test). **e**, Temporal profile of CSCs evoked by moving stimulus of the trained (left) and the opposite direction (right) before and after training. Trace represents the average of CSCs from seven experiments, as in Fig. 2d.

significant directional sensitivity ($n = 9$, data not shown). The requirement of postsynaptic depolarization is reminiscent of hebbian LTP observed at many central synapses[27,28], including LTP of these retinotectal synapses induced by direct electrical stimulation of the retina[18] or by dimming light stimuli[29]. However, step depolarization of the tectal cell (voltage-clamped from −70 to 0 mV, 700 ms), when paired with each training stimulus, was not sufficient to enhance the response to the training stimulus (Fig. 5a). Thus postsynaptic spike-associated depolarization and perhaps other factor(s) are essential for the observed training effect.

In many regions of the brain[27,28], including the developing tectum[18], activity-induced LTP requires activation of NMDA receptors. To test further whether the mechanism underlying changes to the receptive field described here involves NMDA receptor-dependent synaptic plasticity in the tectum, we perfused the tectum locally with the NMDA receptor antagonist D-2-amino-5-phosphonopentanoic acid (APV). The effectiveness of the local perfusion of drugs was shown by the finding that perfusion with CNQX (6-cyano-7-nitroquinoxaline-2,3-dione) abolished fast transient currents associated with moving-bar-induced CSCs, and that perfusion with APV blocked NMDA receptor-mediated synaptic currents induced by electrical stimulation of retinal ganglion cells (Fig. 5b, top panel). Perfusion of APV did not affect significantly the tectal response to each sweep of the moving bar, in terms of either total CSC charge or spiking activity (Fig. 5b, middle and bottom left panels), but it abolished completely direction-specific change in the tectal responses induced by training (Fig. 5b, bottom right panel). Thus, activation of NMDA receptors is required for the induction of direction-sensitive responses, consistent with the blocking effect of APV on LTP of retinotectal synapses[18].

Further analysis was carried out to determine the relative contributions of excitatory and inhibitory inputs to the CSCs evoked by each moving-bar stimulus. On the basis of measurements of the average CSC charge at two different clamping voltages and the reversal potentials for Na^+ and Cl^- currents (see Methods), we found that excitatory glutamate-mediated inputs contributed to about 90% of the total CSC charge at −70 mV (Fig. 5c, left). After training with fast bars, there was selective increase in these excitatory inputs in terms of the total charge of excitatory components of the CSCs (Fig. 5c, right), as well as a significant increase in both the size and the average frequency of excitatory postsynaptic currents (EPSCs) associated with CSCs evoked by test bars of the training direction (Fig. 5d). Taken together, these results suggest that the training had induced a potentiation of glutamate-mediated inputs on these tectal cells.

The observed induction of direction-sensitivity of tectal neurons could result from a strengthening of retinotectal connections made by direction-selective retinal ganglion cells at this early stage of development. Alternatively, it may arise from a training-induced circuit modification within the tectum. In principle, direction-selectivity of a visual neuron can develop through an activity-dependent asymmetric circuit modification that results in excitation of the neuron only when the stimulus of the preferred direction is presented[21–24]. We note that, after training with the moving bar, the profiles of CSCs were asymmetrically altered for responses elicited by stimuli in the trained and the opposite directions (Fig. 5e), suggesting distinct circuit modifications for detection of moving signals in preferred and non-preferred directions. The observed requirement of tectal-cell spiking is consistent with a circuit modification that involves spike-time-dependent modification of retinotectal and/or intra-tectal connections, although training-induced changes in the retina may also occur. Although the precise loci of circuit changes remain to be determined, the rapidity and persistence of receptive field modification shown here illustrate the susceptibility of developing neural circuits to the instructive influence by sensory inputs of specific spatiotemporal patterns. □

Methods

Tadpole preparation and electrophysiology

Xenopus laevis tadpoles of Nieuwkoop and Faber stage 42–45 were anaesthetized with saline containing 0.02% MS222 (Sigma) and secured by insect pins to a sylgard-coated dish, and incubated in HEPES-buffered saline containing (in mM): 115 NaCl, 2 KCl, 10 HEPES, 3 $CaCl_2$, 10 glucose, 1.5 $MgCl_2$, and 0.005 glycine (pH 7.4). For recording, the skin was removed and the brain was split open along the midline to expose the inner surface of the tectum. A low dose of α-bungarotoxin (2 mg ml^{-1}) was applied to the bath to prevent muscle contraction. As shown previously[18], this toxin treatment did not significantly affect the retinotectal responses. The method of perforated-patch, whole-cell recording has been described previously[30]. The micropipettes were made from borosilicate glass capillaries (Kimax), had a resistance in the range of 3–4 MΩ, and were tip-filled with internal solution and then back-filled with internal solution containing 200 mg ml^{-1} amphotericin B. The internal solution contained (in mM): 110 K-gluconate, 10 KCl, 5 NaCl, 1.5 $MgCl_2$, 20 HEPES, 0.5 EGTA (pH 7.3). Experiments were performed at room temperature (22 °C) and the bath was constantly perfused with fresh recording medium at a slow rate (1 ml min^{-1}). Recording was made with a patch-clamp amplifier (Axopatch 200A; Axon Instruments). The whole-cell capacitance was fully compensated and the series resistance (10–20 MΩ) was compensated at 75–80% (lag 60 μs). Signals were filtered at 5 kHz and sampled at 10 kHz using Axoscope software (Axon Instruments). Local perfusion of the tectum was carried out with a glass pipette (opening 30–40 μm) placed near the tectum. All drugs were from Sigma. Concentrations used were: 10 μM CNQX, 10 μM bicuculline, 50 μM D-APV.

For mapping of the receptive field, recordings were made under the reversal potential for Cl^- current ($E_i = -45$ to -60 mV), which was determined by the disappearance and the reversal of spontaneous GABA (γ-aminobutyric acid)-mediated synaptic currents as the holding potential was changed towards more depolarized values. To determine the contribution of excitatory and inhibitory components of stimulus-evoked CSCs, recordings were repeated at two holding potentials (−90 and −70 mV). The Na^+ and Cl^- conductances were determined by the formula $I(t) = (G_e + g_e(t))^*(V - E_e) + (G_i + g_i(t))^*(V - E_i)$, where $I(t)$ is the amplitude of CSCs at time t; $g_e(t)$ and $g_i(t)$ are Na^+ and Cl^- conductances; V is the clamping voltage; E_e and E_i are reversal potentials for Na^+ and Cl^- currents, respectively; and G_e and G_i are leakage conductances (which are negligible). Measurements of $I(t)$ at two voltages (averages of 20 repeats) yielded $g_e(t)$ and $g_i(t)$, and the relative contribution of Na^+ and Cl^- currents to CSCs were calculated. For estimates of changes in EPSCs, fast transients of CSCs were identified by custom-made LabVIEW (National Instruments) software to determine the peak amplitude of individual EPSCs and their frequency. For analysis of spiking patterns, the peak of spikes observed in the tectal responses was identified and the inter-spike intervals were calculated.

Visual stimulation

The tectal cell was patched under visual control and the retina was flattened and stabilized with a glass coverslip after removal of the lens. A small LCD screen (from a virtual reality goggle, Sony, PLM-A35) was mounted on the camera port of the microscope, allowing projection of computer-generated images onto the retina (Fig. 1a). The diameter of the retina was in the range of 250–300 μm and that of the tectal receptive field in the range of 100–200 μm. Visual stimulation and analysis software was custom-made. For receptive field mapping, the entire field for image projection (200 × 200 μm) was divided into a 8 × 7 grid. White squares (corresponding to each element of the grid) were flashed for 1.5 s in a random sequence, with 5-s intervals. For moving-bar stimuli, white bars (20 μm in width at the retina) swept across the screen at a speed of 0.3, 0.2 or 0.1 μm ms^{-1} (fast, medium and slow speed, respectively). For testing tectal responses, bars moving in four orthogonal directions (in the sequence of up, right, down and left) were presented with 10-s intervals, with 3–5 repeats in each testing session. Two or three testing sessions (with 5-min interval) were performed during the control period. In some experiments, responses to two different speeds were tested. The training session consisted of 60 sweeps of a randomly chosen direction (0.2 Hz), or 240 sweeps of four orthogonal directions with a randomized order (0.5 Hz). For random flashing stimulus, white squares of the same width as the moving bar were flashed at random at non-overlapping locations (see example images in Fig. 3c, inset), exposing the retina to the same total amount of light at any given moment, and covering the same total area as the fast-moving bar stimulus. A total of 120 sets of stimuli (0.2 Hz) were applied for training. For rapid mapping of training-induced changes in the receptive field, the image projection field was divided into a set of ten horizontal and ten vertical bars. Each bar was flashed for 1.5 s (at 5-s interval) and the sequence of flashing bars was randomized. After preliminary mapping of the receptive field, the size of the image projection field was sometimes slightly re-adjusted to cover the entire receptive field. The receptive field was then mapped in two sessions (four repeats in each session) before and after training.

Received 6 May; accepted 12 July 2002; doi:10.1038/nature00988.

1. Wiesel, T. N. Postnatal development of the visual cortex and the influence of environment. *Nature* **299,** 583–591 (1982).
2. Katz, L. C. & Shatz, C. J. Synaptic activity and the construction of cortical circuits. *Science* **274,** 1133–1138 (1996).
3. Penn, A. A. & Shatz, C. J. Brain waves and brain wiring: the role of endogenous and sensory-driven neural activity in development. *Pediatr. Res.* **45,** 447–458 (1999).
4. Zhang, L. I. & Poo, M. M. Electrical activity and development of neural circuits. *Nature Neurosci.* **4** Suppl., 1207–1214 (2001).
5. Hubel, D. H. & Wiesel, T. N. Binocular interaction in striate cortex of kittens reared with artificial squint. *J. Neurophysiol.* **28,** 1041–1059 (1965).
6. Meister, M., Wong, R. O., Baylor, D. A. & Shatz, C. J. Synchronous bursts of action potentials in ganglion cells of the developing mammalian retina. *Science* **252,** 939–943 (1991).

7. Penn, A. A., Riquelme, P. A., Feller, M. B. & Shatz, C. J. Competition in retinogeniculate patterning driven by spontaneous activity. *Science* **279,** 2108–2112 (1998).
8. Cynader, M., Berman, N. & Hein, A. Cats reared in stroboscopic illumination: effects on receptive fields in visual cortex. *Proc. Natl Acad. Sci. USA* **70,** 1353–1354 (1973).
9. Schmidt, J. T. & Eisele, L. E. Stroboscopic illumination and dark rearing block the sharpening of the regenerated retinotectal map in goldfish. *Neuroscience* **14,** 535–546 (1985).
10. Weliky, M. & Katz, L. C. Disruption of orientation tuning in visual cortex by artificially correlated neuronal activity. *Nature* **386,** 680–685 (1997).
11. Sharma, J., Angelucci, A. & Sur, M. Induction of visual orientation modules in auditory cortex. *Nature* **404,** 841–847 (2000).
12. von Melchner, L., Pallas, S. L. & Sur, M. Visual behaviour mediated by retinal projections directed to the auditory pathway. *Nature* **404,** 871–876 (2000).
13. Fregnac, Y., Shulz, D., Thorpe, S. & Bienenstock, E. A cellular analogue of visual cortical plasticity. *Nature* **333,** 367–370 (1988).
14. Schuett, S., Bonhoeffer, T. & Hubener, M. Pairing-induced changes of orientation maps in cat visual cortex. *Neuron* **32,** 325–337 (2001).
15. Gaze, R. M., Keating, M. J. & Chung, S. H. The evolution of the retinotectal map during development in *Xenopus*. *Proc. R. Soc. London B* **185,** 301–330 (1974).
16. Holt, C. E. & Harris, W. A. Order in the initial retinotectal map in *Xenopus*: a new technique for labelling growing nerve fibres. *Nature* **301,** 150–152 (1983).
17. Markram, H., Lübke, J., Frotscher, M. & Sakmann, B. Regulation of synaptic efficacy by coincidence of postsynaptic APs and EPSPs. *Science* **275,** 213–215 (1997).
18. Zhang, L. I., Tao, H. W., Holt, C. E., Harris, W. A. & Poo, M. M. A critical window for cooperation and competition among developing retinotectal synapses. *Nature* **395,** 37–44 (1998).
19. Feldman, D. E. Timing-based LTP and LTD at vertical inputs to layer II/III pyramidal cells in rat barrel cortex. *Neuron* **27,** 45–56 (2000).
20. Boettiger, C. A. & Doupe, A. J. Developmentally restricted synaptic plasticity in a songbird nucleus required for song learning. *Neuron* **31,** 809–818 (2001).
21. Abbott, L. F. & Blum, K. I. Functional significance of long-term potentiation for sequence learning and prediction. *Cereb. Cortex* **6,** 406–416 (1996).
22. Zanker, J. M. & Zeil, J. *Motion Vision—Computational, Neural, and Ecological Constraints* (Springer, New York, 2000).
23. Rao, R. P. & Sejnowski, T. J. Predictive learning of temporal sequences in recurrent neocortical circuits. *Novartis Found. Symp.* **239,** 208–229 (2001).
24. Roberts, P. D. Computational consequences of temporally asymmetric learning rules. I. Differential hebbian learning. *J. Comput. Neurosci.* **7,** 235–246 (1999).
25. Mehta, M. R., Barnes, C. A. & McNaughton, B. L. Experience-dependent, asymmetric expansion of hippocampal place fields. *Proc. Natl Acad. Sci. USA* **94,** 8918–8921 (1997).
26. Mehta, M. R., Quirk, M. C. & Wilson, M. A. Experience-dependent asymmetric shape of hippocampal receptive fields. *Neuron* **25,** 707–715 (2000).
27. Bliss, T. V. P. & Collingridge, G. L. A synaptic model of memory: long-term potentiation in the hippocampus. *Nature* **361,** 31–39 (1993).
28. Malenka, R. C. & Nicoll, R. A. Long-term potentiation—a decade of progress? *Science* **285,** 1870–1874 (1999).
29. Zhang, L. I., Tao, H. & Poo, M. Visual input induces long-term potentiation of developing retinotectal synapses. *Nature Neurosci.* **3,** 708–715 (2000).
30. Rae, J., Cooper, K., Gates, P. & Watsky, M. Low access resistance perforated patch recordings using amphotericin B. *J. Neurosci. Methods* **37,** 15–26 (1991).

Acknowledgements

This work was supported by grants from NSF and NIH. F.E. was supported in part by a long-term fellowship from the Human Frontier Science Program.

Competing interests statement

The authors declare that they have no competing financial interests.

Correspondence and requests for materials should be addressed to M.-m.P. (e-mail: mpoo@uclink.berkeley.edu).

Dendrite growth increased by visual activity requires NMDA receptor and Rho GTPases

Wun Chey Sin, Kurt Haas, Edward S. Ruthazer & Hollis T. Cline

Cold Spring Harbor Laboratory, Cold Spring Harbor, New York 11724, USA

Previous studies suggest that neuronal activity may guide the development of synaptic connections in the central nervous system through mechanisms involving glutamate receptors and GTPase-dependent modulation of the actin cytoskeleton[1–7]. Here we demonstrate by *in vivo* time-lapse imaging of optic tectal cells in *Xenopus laevis* tadpoles that enhanced visual activity driven by a light stimulus promotes dendritic arbor growth. The stimulus-induced dendritic arbor growth requires glutamate-receptor-mediated synaptic transmission, decreased RhoA activity and increased Rac and Cdc42 activity. The results delineate a role for Rho GTPases in the structural plasticity driven by visual stimulation *in vivo*.

We used *in vivo* time-lapse imaging of single optic tectal neurons in *Xenopus* tadpoles to test the function of visual activity in neuronal development. We compared the dendritic arbor growth rates of individual tectal neurons during a 4-h period with a visual stimulus to a preceding 4-h period in the absence of light. This imaging protocol allows the comparison of dendritic arbor structures of the same neurons over time and therefore provides a sensitive measure of structural plasticity. Visual stimulation significantly enhanced dendritic arbor elaboration compared with growth rates in the preceding 4-h period in the dark (Fig. 1a, b; see also Supplementary Table 1). Neurons from animals exposed to visual stimulus throughout the 8-h protocol maintained a constant rate of dendritic arbor elaboration (Fig. 1b; see also Supplementary Fig. 1 and Table 1). This indicates that growth rates do not change with longer periods of stimulation. Another set of animals was exposed to visual stimulus within the first 4-h period and then returned to the dark

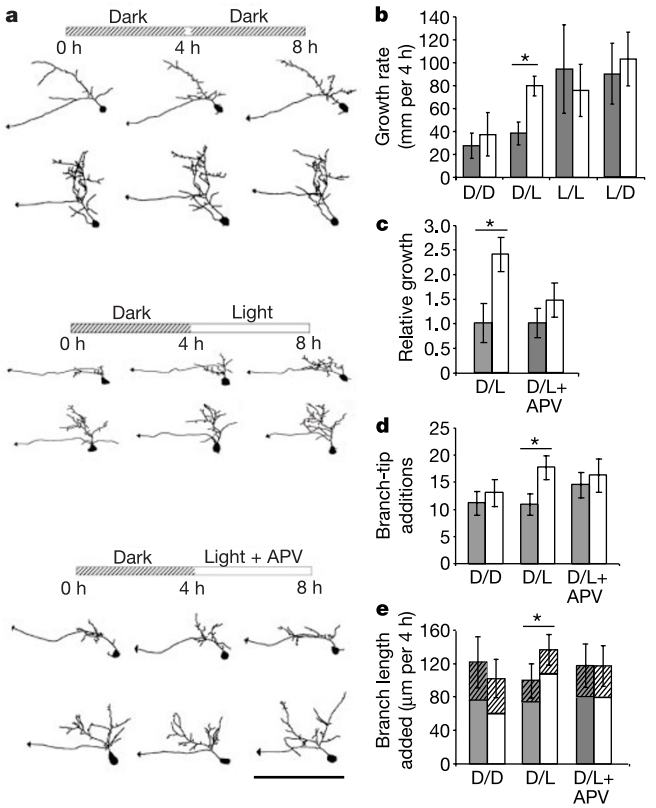

Figure 1 Visual stimulation *in vivo* promotes dendritic arbor growth by a glutamate-receptor-dependent mechanism. **a**, Drawings of neurons imaged three times at 4-h intervals. Two examples are shown for each treatment. Animals were placed in a dark chamber for 4 h (dark) or a chamber with a light stimulus for 4 h (light) in the presence or absence of APV as depicted by the bar over the neurons. Arrowheads identify efferent axons in this and subsequent figures. Scale bar, 100 μm. **b**, Quantification of dendritic arbor growth rates during 4 h in the dark (D) or with visual stimulation (L). **c**, Dendritic arbor growth rates normalized to the growth rate in the 0–4 h period in the dark (D). **d**, Quantification of branch-tip additions. **e**, Contribution of new branches or branch extension (hatched, top region) to increased branch length. Asterisk, $P < 0.05$.